An efficient synthetic access to new uracil-alditols bearing a porphyrin unit and biological assessment in prostate cancer cells

Cristina J. Dias[a], Inês Sardo[b], Nuno M. M. Moura*[a], Juliana Felgueiras[b,c], M. Graça P. M. S. Neves[a], Margarida Fardilha[b], M. Amparo F. Faustino*[a]

[a] *QOPNA & LAQV-REQUIMTE, Department of Chemistry, University of Aveiro, Aveiro, Portugal*

[b] *iBiMED - Institute of Biomedicine, Department of Medical Sciences, University of Aveiro, Aveiro, Portugal*

[c] *Cancer Biology and Epigenetics Group, IPO Porto Research Center (CI-IPOP), Portuguese Oncology Institute of Porto (IPO Porto), Porto, Portugal*

*E-mail: nmoura@ua.pt; faustino@ua.pt

Abstract

An efficient access to porphyrin derivatives bearing uracil-alditol moieties at the β-pyrrolic position was developed. The synthetic strategy involved a hetero Diels-Alder reaction between uracil-alditol based orthoquinodimethanes using 2-vinyl-5,10,15,20-tetraphenylporphyrin as the scaffold. The preliminary evaluation of their photodynamic effectiveness in prostate cancer cells suggests that the adducts **4-Xyl** and **4-Gal** are promising photodynamic agents.

Keywords

Porphyrin derivatives, uracil-alditols, photodynamic therapy, prostate cancer

1. Introduction

Porphyrin macrocycles are well known by their role in important biological processes, such as respiration and photosynthesis, but also by their wide number of applications in different fields like medicine, materials science and biology [1,2]. These macrocycles have chemical, photophysical and biological properties that can be easily modulated through functionalization in order to improve their efficiency as catalysts, sensors, dyes for dye sensitizer solar cell (DSSC) devices or as therapeutic agents among other applications [2–14]. One of the most promising achievements involving porphyrin derivatives is related to their use as photosensitizers (PS) in Photodynamic Therapy (PDT) [15]. PDT has been used with success in the treatment of various oncological and non-oncological diseases such as bacterial infections and some of the clinically approved PS are porphyrin-based [15–20]. PDT continues to gain space as an alternative or

adjunctive treatment modality for various cancers including prostate cancer in order to reduce the possible resistance development and minimize undesirable side effects [21]. Prostate cancer is one of the most common malignancies in male worldwide. Although the current treatment options are quite effective in the management of local disease, tumors eventually become castration-resistant and progress to advanced metastatic stages to which no efficient treatment is hitherto available. The successful application of PDT as a focal therapy in prostate cancer models has been reported in several studies, either alone or in combination with other treatments [21]. PDT combines visible light, molecular oxygen and a non-toxic dye, known as photosensitizer, to produce reactive oxygen species (ROS), mainly singlet oxygen ($^1O_2$), which will induce tissue damage, and consequently, leads to cell death [15,16,22,23]. The possibility to obtain better porphyrinic systems for a specific application through the adequate functionalization of the macrocycle core has been an important field of research. Under this context, the conjugation of different synthons with recognized biological functions is being considered a good approach [15,24,25]. Among the wide range of nitrogen heterocycles with therapeutic potential is uracil. It is considered a lead compound and an important platform for further chemical modifications in order to obtain new compounds with better biological performance, namely antitumoral and antiviral activities [26–28].

Considering the properties of uracils and porphyrins, the construction of porphyrin systems with uracil units has aroused interest of the scientific community in the last decade. However, there are still few studies that explore the conjugation of these two entities. Drain and coworkers designed supramolecular systems through complementary hydrogen bonds based on porphyrins bearing uracil units at *meso*-positions (Fig. 1a) [29]. Takeoka and coworkers [30] developed a porphyrin functionalized at two opposite *meso*-positions with 6-methyl uracil units (Fig. 1b) that was able, depending on the addition of a melanin derivative, to afford atropisomers capable to be organized supramolecularly in distinct ways [30]. Oliveira and co-workers [31] reported the access to β-fused uracil-porphyrin conjugates by tetramerization of adequate uracil-pyrroles (Fig. 1c). These derivatives proved to be emissive and good singlet oxygen producers, fundamental features to be considered as PSs in PDT and for photodiagnosis [31]. Jingchao and coworkers [32] reported the access to several porphyrins as free-bases and as metalloporphyrins containing *L*-phenylalanine and/or 1-carboxymethyl-5-fluorouracil as functional substituents with interesting photophysical properties and photodynamic activity. The *in vitro* phototoxic assessment against human esophageal cancer cell line Ec9706 demonstrated that the phototoxicity enhances by the introduction of one or two uracil unities relatively to the precursor (Fig. 1d) [32].

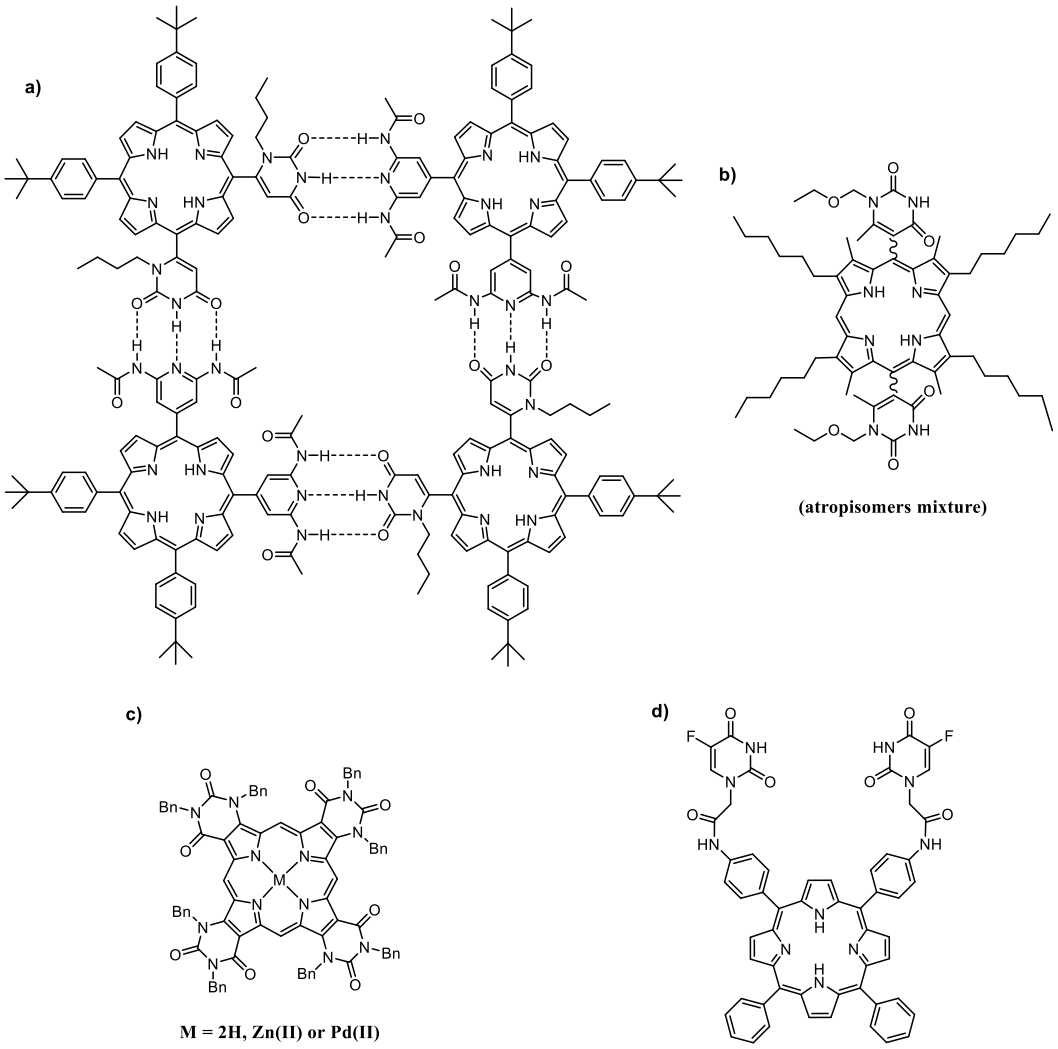

Fig. 1. Some structures of porphyrin systems with uracil units reported in literature from **(a)** [29]; **(b)** [30]; **(c)** [31] and **(d)** [32].

It is well known that some PSs show low selectivity to target cells, which will lead in certain cases to undesirable side-effects. In order to promote the selective uptake of PS by cancer cells, PSs entities have been conjugated with several biomolecules, such as monoclonal antibodies, peptides, epidermal growth factor, low-density lipoproteins, and carbohydrates [15]. Under this context, the conjugation of carbohydrates to PS is particularly relevant. The presence of these biomolecules in the porphyrin core can confer a better solubility to the resulting PS in physiologic medium, and also to provide selectivity as a result of the presence of overexpressed carbohydrates receptors (e.g. galectins) on the surface of tumour cells. These receptors will allow an interaction between the PS-carbohydrate conjugate and the target cell resulting in a higher accumulation of the PS in the tumour cell, making these conjugates suitable for PDT treatments at lower therapeutic doses [25,33–38].

Considering that both units, uracil and carbohydrate, could give rise to compounds with a better photodynamic performance towards cancer cells we envisage the possibility to decorate a porphyrin with

both entities by recurring to the uracil-alditols (scheme 1) reported by Palasz *et al.* [39]. These authors tested the reactivity of these orthoquinodimethanes using enol-ethers as dienophiles. Based on our expertise on cycloaddition reactions involving porphyrins [40–43] we decide to select the 2-vinyl-5,10,15,20-tetraphenylporphyrin (**β-vinylTPP**) as the dienophile [41,42]. So, in this work, it is reported the advantage of an inverse electron demand hetero Diels-Alder transformation to give access for the first time to new porphyrin derivatives bearing uracil-alditol moieties. Preliminary studies concerning the photodynamic efficiency of these conjugates against prostate cancer cell line (PC-3 cell line) will be also discussed.

2. Experimental

2.1. General remarks

All commercial chemicals were used as supplied and were purchased from Sigma-Aldrich or Merck. The solvents were purified or dried according to the literature procedures [44]. ^{1}H and ^{13}C solution NMR spectra were recorded on Bruker Avance 300 (300.13 and 75.47 MHz, respectively) and 500 (500.13 and 125.76 MHz, respectively). Tetramethylsilane (TMS) was used as an internal standard, chemical shifts (δ) are expressed in part per million (ppm) and the coupling constants (J) in Hertz (Hz). Unequivocal ^{1}H assignments were made using two-dimensional COSY ($^{1}H/^{1}H$). ESI spectra were recorded on a Micromass Q-Tof spectrometer operating in positive mode. Mass spectra HRMS were recorded on a LTQ Orbitrap XL mass spectrometer (Thermo Fischer Scientific, Bremen, Germany) using chloroform as solvent. UV-Vis spectra were recorded on an UV-2501-PC Shimadzu spectrophotometer, and emission spectra were recorded on a HORIBA-Jobin-Yvon Fluoromax 3 spectrofluorimeter, using DMF as solvent and at 293 K. Preparative thin-layer chromatography (TLC) was carried out on 20x20 cm glass plates coated with silica gel 60 (Merck, 0.5 mm). Analytical TLC was carried out on precoated sheets with silica gel 60 (Merck, 0.2 mm).

2.2 Synthesis

2.2.1. Synthesis of 2-vinyl-5,10,15,20-tetraphenylporphyrin (1)

2-Vinyl-5,10,15,20-tetraphenylporphyrin (**β-vinylTPP**, **1**) was prepared according to literature procedures and the spectroscopic data are in accordance with the data reported (see Fig. S1 and Fig. S2) [45,46].

2.2.2. Synthesis of uracil-alditols 2-Xyl and 2-Gal

The uracil-alditols **2-Xyl** and **2-Gal** were prepared in two steps according to the literature procedure. Their spectroscopic data are in accordance with the literature (see Fig. S3-S6, SI) [39,47].

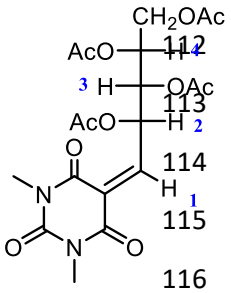

Compound **2-Xyl:** ^{1}H NMR (300.13 MHz, $CDCl_3$): δ 2.06 (3H, s, OAc), 2.10 (3H, s, OAc), 2.11 (3H, s, OAc), 2.19 (3H, s, OAc), 3.340 (3H, s, *N*-CH_3), 3.344 (3H, s, *N*-CH_3), 4.14 (1H, dd, *J* = 5.8 and 12.3 Hz, H-5), 4.38 (1H, dd, *J* = 3.9 and 12.3 Hz, H-5), 5.39-5.44 (1H, m, H-4), 5.68 (1H, dd, *J* = 2.8 and 7.0 Hz, H-3), 6.48 (1H, dd, *J* = 2.8 and 7.0 Hz, H-2), 7.45 (1H, d, *J* = 7.0 Hz, H-1) ppm. ESI-MS(+):m/z calcd for $C_{19}H_{24}N_2O_{11}Na$ $[M+Na]^+$ 479.13; found 479.1.

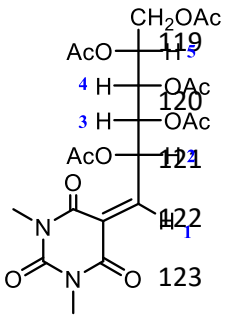

Compound **2-Gal:** ^{1}H NMR (300.13 MHz, $CDCl_3$): δ 2.04 (6H, s, OAc), 2.05 (3H, s, OAc), 2.16 (3H, s, OAc), 2.19 (3H, s, OAc), 3.33 (3H, s, *N*-CH_3), 3.38 (3H, s, N-CH_3), 3.90 (1H, dd, *J* = 7.5 and 11.6 Hz, H-6), 4.31 (1H, dd, *J* = 5.0 and 11.6 Hz, H-6), 5.33-5.37 (1H, m, H-5), 5.56 (1H, dd, *J* = 2.0 and 9.9 Hz, H-4), 5.68 (1H, dd, *J* = 1.9 and 9.9 Hz, H-3), 6.39 (1H, dd, *J* = 1.9 and 6.9 Hz, H-2), 7.40 (1H, d, *J* = 6.9 Hz, H-1) ppm. ESI-MS(+):m/z calcd for $C_{22}H_{28}N_2O_{13}Na$ $[M+Na]^+$ 551.15; found 551.2.

2.2.3. Synthesis of protected porphyrin-uracil-alditols conjugates 3-Xyl and 3-Gal

Porphyrin **β-vinylTPP 1** (20 mg) and compounds **2-Xyl** or **2-Gal** (2 eq.) were dissolved in dry (2 mL) toluene and the reaction mixture was maintained under stirring for 4 h at 120 °C or for 15 h at room temperature. After this time, the solvent was evaporated under reduced pressure. The crude was purified by thin-layer chromatography using dichloromethane-methanol (1%) mixture as eluent.

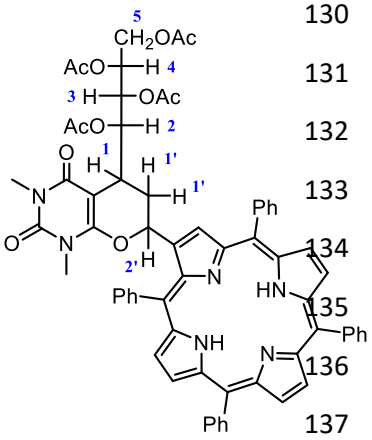

Compound **3-Xyl:** 76% yield at 120 °C *vs* 53% at room temperature. ^{1}H NMR (300.13 MHz, $CDCl_3$): δ -2.72 (2H, s, N*H*), 1.90 (3H, s, OAc), 1.93 (3H, s, OAc), 1.94 (3H, s, OAc), 2.28-2.40 (5H, m, H-1' e OAc), 2.75-2.82 (1H, m, H-1), 3.28 (3H, s, *N*-CH_3), 3.35 (3H, s, *N*-CH_3), 3.97 (1H, dd, *J* = 7.1 and 11.5 Hz, H-5), 4.26 (1H, dd, *J* = 5.4 and 11.5 Hz, H-5), 4.82 (1H, dd, *J* = 0.6 and 10.5 Hz, H-2'), 5.22 (1H, dd, *J* = 2.7 and 8.8 Hz, H-3), 5.47-5.53 (1H, m, H-4), 6.10 (1H, dd, *J* = 1.3 and 8.8 Hz, H-2), 7.61-7.66 (1H, m, H-*m,p*-Ph), 7.73-7.82 (10H, m, H-*m,p*-Ph), 7.97-8.00 (1H, m, H-*m,p*-Ph), 8.08 (1H, d, *J* = 7.6 Hz, H-*o*-Ph), 8.18-8.25 (7H, m, H-*o*-Ph), 8.72 (1H, d, *J* = 4.9 Hz, H-β), 8.79-8.95 (6H, m, H-β) ppm. ^{13}C NMR (125.76 MHz, $CDCl_3$): δ 20.56, 20.64, 20.7, 20.9, 21.1, 21.2, 27.9, 28.1, 28.7, 28.8, 29.7, 31.9, 32.9, 62.2, 62.6, 68.2, 68.9, 69.18, 69.21, 70.75, 70.82, 85.05, 87.12,

119.2, 120.3, 120.4, 120.6, 120.7, 124.0, 126.8, 126.9, 127.3, 127.6, 127.9, 128.0, 129.5, 133.4, 133.7, 134.56, 134.64, 134.8, 134.9, 134.9, 141.3, 141.6, 141.7, 142.0, 142.3, 151.0, 156.6, 158.1, 162.1, 169.4, 170.0, 170.6, 171.0 ppm. UV-Vis (DMF): $\lambda_{máx}$ (log Ɛ): 419 (5.62), 516 (4.51), 554 (4.15), 592 (4.04), 647 (3.89) nm. HRMS-ESI(+): *m/z* calcd for $C_{65}H_{57}N_6O_{11}$ $[M+H]^+$ 1097.4080; found 1097.4090.

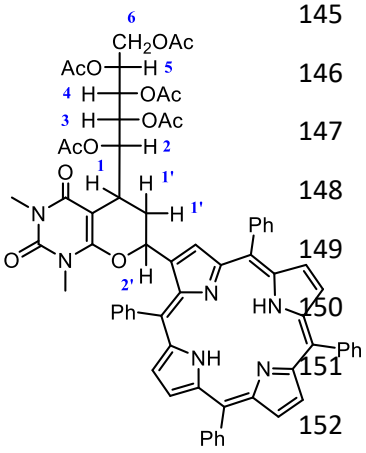

Compound **3-Gal:** 93% yield at 120 °C *vs* 47% at room temperature. ^{1}H NMR (300.13 MHz, $CDCl_3$): δ -2.74 (2H, s, N*H*), 1.78-2.23 (15H, m, 5 OAc), 2.24-2.32 (2H, m, H-1'), 2.90-3.00 (1H, m, H-1), 3.21-3.43 (6H, m, 2 *N*-CH_3), 3.81-3.90 (1H, m, H-6), 4.23-4.35 (1H, m, H-6), 4.56-4.65 (1H, m, H-2'), 5.13-5.27 (2H, m, H-4 and H-5), 5.44-5.56 (1H, m, H-3), 5.93-6.02 (1H, m, H-2), 7.53-7.91 (12H, m, H-*m,p*-Ph), 7.99-8.37 (8H, m, H-*o*-Ph), 8.55-8.95 (7H, m, H-β) ppm. ^{13}C NMR (125.76 MHz, $CDCl_3$): *δ* 20.7, 20.90, 20.92, 21.2, 28.0, 28.7, 29.1, 29.3, 29.7, 30.2, 31.6, 35.2, 62.2, 62.6, 67.6, 67.7, 68.6, 70.8, 85.8, 88.4, 119.1, 120.3, 120.4, 120.5, 120.6, 120.7, 126.8, 126.9, 127.3, 127.9, 128.0, 128.9, 129.7, 133.3, 133.5, 134.56, 134.63, 141.3, 141.5, 141.6, 141.9, 142.0, 142.2, 142.3, 150.9, 151.0, 157.9, 162.7, 162.8, 169.6, 169.7, 169.9, 170.0, 170.3, 170.5, 170.6 ppm. UV-Vis (DMF): $\lambda_{máx}$ (log Ɛ): 420 (5.73), 515 (4.50), 552 (4.16), 592 (4.04), 650 (3.92) nm. HRMS-ESI(+): *m/z* calcd for $C_{68}H_{61}N_6O_{13}$ $[M+H]^+$ 1169.4291; found 1169.4304.

2.2.4. Unprotected porphyrin-uracil-alditol conjugates 4-Xyl and 4-Gal

Sodium methoxide (2 eq.) was added to conjugates **3-Xyl** or **3-Gal** (10 mg) dissolved in of a mixture of methanol and tetrahydrofuran (THF) (2 mL, 1:1). The reaction was stirred at 50 °C and its evolution was controlled by TLC. When no starting material was observed in the TLC, the reaction was allowed to cool down and it was added a solution of citric acid. The desired product was extracted with dichloromethane, washed with water and crystalized in dichloromethane:hexane.

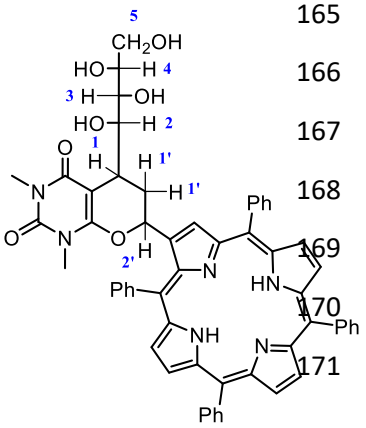

Compound **4-Xyl**: 75% yield. ^{1}H NMR (300.13 MHz, $CDCl_3$): δ -2.69 (2H, m, N*H*) 2.39-3.31 (3H, m, H-1 and H-1'), 3.35 (3H, s, N-CH_3), 3.38 (3H, s, N-CH_3), 4.56-5.87 (6H, m, H-2, H-3, H-4, H-5 and H-2'), 7.57-7.91 (12H, m, H-*m,p*-Ph), 8.00-8.41 (8H, m, H-*o*-Ph), 8.58-8.97 (7H, m, H-β) ppm. ^{13}C NMR (125.76 MHz, $CDCl_3$): δ 14.2, 19.7, 22.7, 25.6, 28.0, 28.4, 28.5, 29.06, 29.13, 29.4, 29.7, 30.3, 32.0, 32.9, 34.4, 36.7, 49.0, 63.6, 64.1, 68.0, 70.5, 70.9, 72.7, 73.0, 73.1, 73.7, 74.4, 76.8, 77.0,

77.3, 77.9, 80.7, 85.5, 89.3, 118.8, 120.4, 120.6, 120.7, 126.8, 126.9, 127.0, 127.4, 127.8, 127.9, 128.1, 128.6, 129.0, 133.6, 133.9, 134.55, 134.63, 141.6, 142.0, 142.2, 143.2, 150.4, 150.5, 157.70, 157.73, 158.3, 165.36, 165.40 ppm. UV-Vis (DMF): $\lambda_{máx}$ (log Ɛ): 419 (5.44), 514 (4.54), 553 (4.19), 591 (4.08), 649 (3.88) nm. MS (MALDI): *m/z* 929.3 $[M+H]^+$. HRMS-ESI(+): *m/z* calcd for $C_{57}H_{49}N_6O_7$ $[M+H]^+$ 929.3657; found 929.3667.

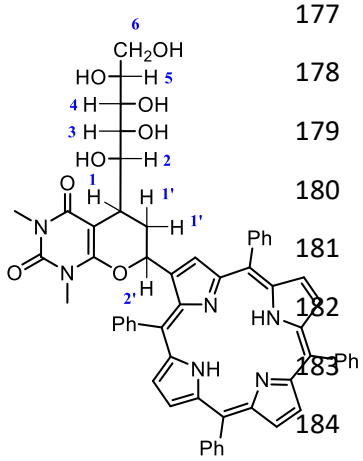

Compound **4-Gal**: 63% yield. ^{1}H NMR (300.13 MHz, $CDCl_3$): δ -2.75 (2H, m, N*H*) 2.40-4.11 (9H, m, N-CH_3, H-1 and H-1'), 4.47-5.82 (7H, m, H-2, H-3, H-4, H-5, H-6 and H-2'), 7.49-7.88 (12H, m, H-*m,p*-Ph), 8.03-8.43 (8H, m, H-*o*-Ph), 8.56-9.03 (7H, m, H-β) ppm. ^{13}C NMR (125.76 MHz, $CDCl_3$): δ 22.7, 23.9, 25.6, 28.0, 29.0, 29.4, 29.5, 29.7, 34.6, 67.4, 68.0, 72.1, 76.8, 77.0, 77.3, 119.0, 119.5, 120.5, 120.6, 126.7, 126.8, 126.9, 127.8, 127.9, 133.5, 133.9, 134.6, 140.0, 141.6, 141.9, 142.2, 143.2, 157.6, 171.6 ppm. UV-Vis (DMF): $\lambda_{máx}$ (log Ɛ): 419 (5.56), 515 (4.54), 551 (4.19), 591 (4.07), 648 (3.87) nm. MS (MALDI): *m/z* 959.3 $[M+H]^+$. HRMS ESI (+): *m/z* calcd for $C_{58}H_{51}N_6O_8$ $[M+H]^+$ 959.3763; found 959.3777.

2.3. Characterization studies

2.3.1. Singlet oxygen generation

A stock solution of each porphyrin-uracil-alditol conjugate (**3-Xyl**, **3-Gal**, **4-Xyl** and **4-Gal**) at 0.1 mM in DMF and a 10 mM stock solution of 1,3-diphenylisobenzofuran (DPiBF) in DMF were prepared. In a quartz cell, aliquots of 2.5 mL of compound **3-Xyl**, **3-Gal**, **4-Xyl**, **4-Gal** or 5,10,15,20-tetraphenylporphyrin (**TPP**) (used as reference) at the concentration of 0.5 µM and DPiBF at the concentration of 50 µM were stirred at room temperature and irradiated with a LED array (5 x 10 LEDs; λ = 630 ± 20 nm) at an irradiance of 4.0 mW cm^{-2}. The singlet oxygen production was monitored by measuring the decreasing of DPiBF absorbance at 415 nm, at intervals of 60 s, during 600 s of irradiation.

2.3.2. Emission properties

The fluorescence quantum yields (ΦF) of the conjugates **3** and **4** were obtained using a solution of **TPP** in DMF as standard (Φ_F = 0.11, in DMF). All the measurements were recorded in DMF at 293 K, in quartz cells (3). In all measures, it was recorded the absorption spectra of the compound and of the standard, and samples were excited at the wavelength of the absorbance crossing point of both. The absorbance at this crossing point was kept in the range 0.02-0.04 and the excitation occurred in the Soret band region.

Fluorescence quantum yield was calculated from equation 1 (Eqn. 1), where Φ_F^{Std} is the fluorescence quantum yield of TPP (standard), and A and A_{Std} are the integrated area under the fluorescence curves of the compounds and the standard, respectively.

$$Eqn.\ 1) \qquad \Phi_F = \Phi_F^{Std} \frac{A}{A_{Std}}$$

2.4. Biological studies

2.4.1. Cell Culture

The human prostate cell line PC-3 (prostatic adenocarcinoma cells, grade IV, isolated from bone metastasis of a 62-years-old Caucasian man) used was kindly provided by Dr. Rui Medeiros, University of Porto, Portugal. The cells were grown as monolayers in Roswell Park Memorial Institute (RPMI) 1640 medium, supplemented with 10% fetal bovine serum (FBS) and 1% antibiotics (penicillin and streptomycin mixture). Cells were maintained in a MCO-170AICUV incubator (Panasonic Healthcare Co., LTD – Hamburg, Germany) at 37 ºC in a humidified 5% CO_2 atmosphere.

2.4.2. Stock solutions

Stock solutions of 10 mM of conjugates **3-Xyl**, **3-Gal**, **4-Xyl** and **4-Gal** were prepared in dimethyl sulfoxide (DMSO) and were kept protected from light at room temperature. The final concentrations of the conjugates used in the biological studies were obtained by further dilution of the stock solutions in RPMI-1640 medium. In all assays, the highest concentration of DMSO used per well was 1% (v/v).

2.4.3. Light source

Irradiations were performed using a Back-Light LED-Setup (provide by AG Photobiophysik, Humboldt-Universität zu Berlin, Germany), which delivers white light (400-800 nm). The LED-Setup was covered with a red filter (λ = 630 ± 20 nm) and cells were exposed to red light at an irradiance of 1.28 mW cm^{-2}, measured with an energy power meter Coherent FieldMaxII-Top combined with a Coherent PowerSens PS19Q energy sensor.

2.4.4. Cytotoxic and phototoxic assays

PC-3 cells (7 500 cells per well) were seeded in a 96-well plate (100 µL) for 24 h at 37 °C in a humidified 5% CO_2 atmosphere. The compounds were added at different concentrations (1.0, 10 and 100 µM) to the cells

and incubated in the dark for 4 h. Cells without treatment and cells treated with 1% DMSO were used as controls. After this period, the plate was positioned on a Back-Light LED-Setup and irradiated for 20 min. Then, the culture medium was replaced by fresh medium and cells were incubated for 24 h. Four hours before the endpoint of the assay, 10 µL of AlamarBlue reagent (ThermoFisher, Massachusetts, USA) was added to each well. Cell viability was assessed by measuring the absorbance, at 570 and 600 nm, using a microplate reader (Tecan Infinite® 200 Pro series, Männedorf, Switzerland). Cytotoxic assays were performed using a similar protocol but protected from light. At least three independent assays were conducted for each experimental condition.

2.5 Statistical Analysis

The statistical significance of cell viability assays was assessed by Mann-Whitney tests of the equality of means for independent samples and was conducted using IBM SPSS Statistics Software 22. The significance level was set at 0.05.

3. Results and Discussion

3.1. Synthesis of porphyrin-uracil-alditol conjugates 3 and 4

The synthetic strategy used to prepare the new porphyrinic derivatives **3** and **4** decorated with uracil-alditols units is summarized in scheme 2. As it was mentioned above, the key step of the approach was the hetero Diels-Alder reaction between the orthoquinodimethanes uracil-alditols **2** and the 2-vinyl-5,10,15,20-tetraphenylporphyrin (**β-vinylTPP**, **1**) selected as the dienophile. The heterodienes **2-Xyl** and **2-Gal** were prepared according to the methodology reported by Palasz *et al.*, [39] and involved in a first step the Knoevenagel condensation between the sugar moieties D-(+)-xylose and D-(+)-galactose with 1,3-dimethylbarbituric acid. After carbohydrate acetylation and ring-opening in the presence of $ZnCl_2$, compounds **2-Xyl** and **2-Gal** were obtained in 55% and 37% yield, respectively (scheme 1 and see in SI Fig. S3-S6) [39,47]. The **β-vinylTPP** was prepared from the Wittig reaction of 2-formyl-5,10,15,20-tetraphenylporphyrinatozinc(II) with the ylide generated *in situ* by treatment of methyltriphenylphosphonium bromide with NaH, followed by demetalation with trifluoroacetic acid [45,46].

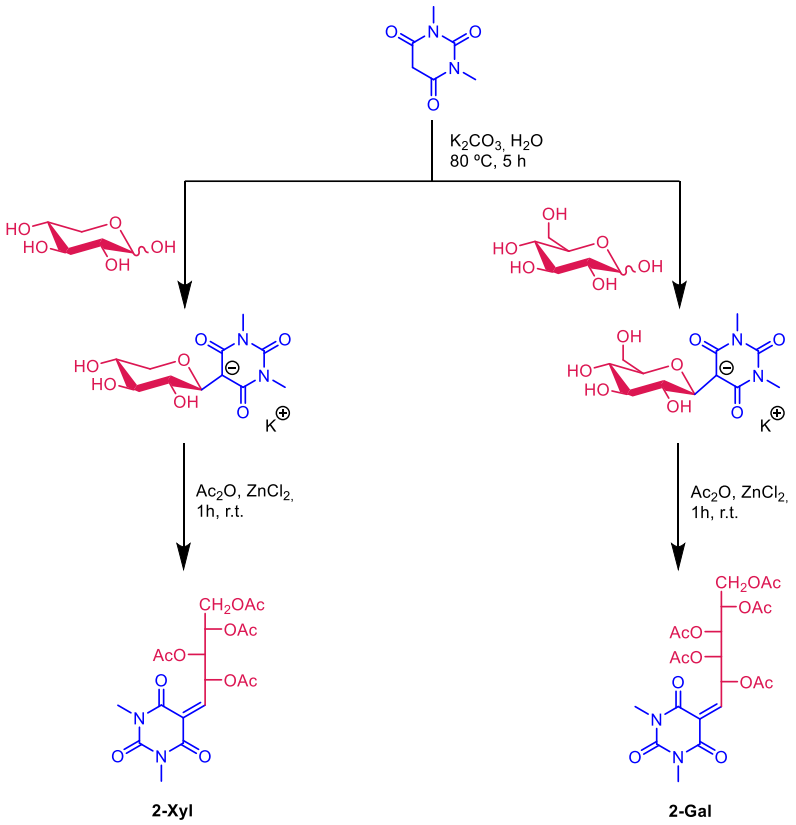

Scheme 1. Synthetic strategy used in the preparation of uracil-alditols **2-Xyl** and **2-Gal**.

The reaction between the **β-vinylTPP** (**1**) and the uracil-alditols **2-Xyl** and **2-Gal** was carried out in dry toluene at room temperature and at 120 °C, affording in both cases the protected cycloadducts **3-Xyl** and **3-Gal** in moderate to excellent yields. The best results in terms of reaction time and yields were attained at 120 °C. At this temperature, after 4h, compound **3-Xyl** was isolated in 76% yield at 120 °C *vs* 53% at room temperature. For cycloadduct **3-Gal** the achievement was even better since it was obtained in 93% yield at 120 °C *vs* 47% at room temperature. The low yield observed for both adducts (**3-Xyl** and **3-Gal**) when the reaction was performed at room temperature is probably related with the electron-deficient behaviour of the hetero-diene that, consequently, requires higher energy to participate in the Hetero-Diels-Alder reaction. As expected, due to the high number of chiral centres, these conjugates were obtained as a mixture of diastereoisomers.

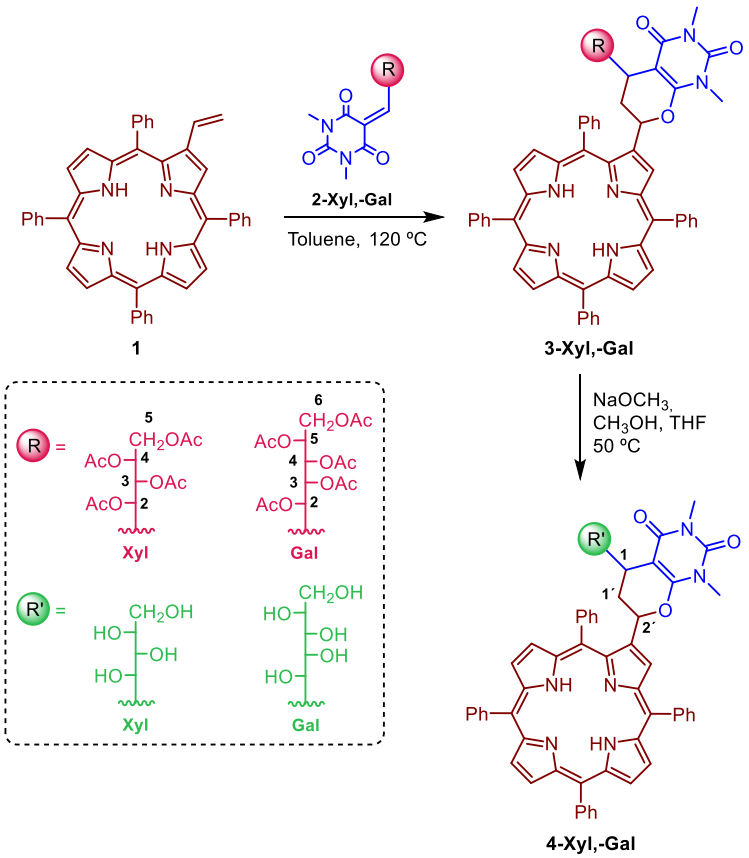

Scheme 2. Synthetic route for the preparation of porphyrin-uracil-alditol conjugates **3** and **4**.

The formation of these cycloadducts was confirmed by adequate spectroscopic techniques (see SI). In their ^{1}H NMR spectra (see Fig. S7 and Fig. S10, SI) the characteristic proton resonances of the porphyrin nucleus appear in the aromatic region with the expected pattern of a mono-substituted porphyrin (seven β-pyrrolic protons at *ca.* δ 8.9-8.6 ppm); the signals of the *meso*-phenyl protons appear as two multiplets at *ca.* δ 8.4-8.0 (*ortho*-H) and 7.9-7.5 ppm (*meta*- and *para*-H). The resonances of the porphyrinic vinyl protons (three doublet of doublets at δ 6.4, 5.9 and 5.2 ppm) and of the alditol moiety at δ 7.45 ppm do not appear in cycloadducts ^{1}H NMR spectra confirming the success of the coupling. The protons H-1´ and H-2´ due to the formation of the new heterocyclic unit appear in the range of δ 2.4-2.2 and 4.8-4.5 ppm, respectively. The evidence of the proposed adduct was confirmed by the 2D COSY (^{1}H/^{1}H) spectrum (Fig. S8), where the signal due to the resonance of the H-2' correlates with the a doublet of doublets signal due to the resonance of CH_2 (H-1') that correlates with H-1.The signals due to the resonance of acetate protons from the sugar protecting groups and of the methyl protons attached to the uracyl nitrogen atoms appear in the range of δ 2.4-1.7 and of 3.4-3.2 ppm, respectively, the same region found in the alditol ^{1}H NMR spectra before coupling. Moreover, the molecular formula of these compounds was further confirmed by high

resolution mass spectrometry ESI(+)-HRMS analysis showing the peak corresponding to the respective $[M+H]^+$ molecular ion (see Fig. S15 and S16, SI).

Knowing that the solubility of a compound in a physiological medium is an important feature to take into account for its potential application as a PS in PDT, in the final synthetic strategy step, it was considered the deprotection of the hydroxyl groups in cycloadducts **3** (Scheme 2). This reaction was carried out for both adducts in tetrahydrofuran at 50 °C, in the presence of sodium methoxide, affording the unprotected and more polar cycloadducts **4-Xyl** and **4-Gal** in 75% and 63% yield, respectively. The analysis of their ^{1}H NMR spectra revealed the disappearance of the acetyl groups signals confirming the success of the deprotection step (see Fig. S13 and S14, SI). The HRMS spectra of **4-Xyl** and **4-Gal** are also in accordance with the predicted structure for the $[M+H]^+$ molecular ion (see Fig. S17 and S18, SI).

3.2. Photophysical characterization and singlet oxygen generation

The photophysical characterization of cycloadducts **3** and **4** was performed in DMF at 293 K and the most important photophysical data are presented in Table 1 (see also in SI Fig. S19 and S20). As an example, in Fig. 2 is represented the absorption, excitation and emission spectra of the porphyrin-uracil-alditol conjugate **3-Xyl**. All the studied cycloadducts **3-Xyl,-Gal** and **4-Xyl,-Gal** present the typical absorption pattern of an ethio-type porphyrin macrocycle due to π-π* transitions [48]. The introduction of the uracil-alditol units in the porphyrin did not affect significantly the absorption properties of the porphyrinic macrocycle when compared with the precursor **β-vinylTPP 1** displaying the strong Soret band absorption at *ca.* 420 nm (Table 1) and the less intense but well-defined Q bands between *ca.* 514-650 nm (see Fig. 2 and Fig. S19, SI). All conjugates in DMF are also emissive compounds as their precursor (Fig. 2 and Fig. S20, SI) and present two bands centred at *ca.* 655 and 716 nm, where the first vibrational mode of the fluorescence is much more pronounced than the second one. This is a typical behaviour of *meso*-tetraarylporphyrins and the emission bands are attributed to Q_x (0-0) and Q_x (0–1) transitions due to a nearly unchanged vibronic state upon excitation [49,50]. The resemble between the absorption and the excitation spectra indicates the absence of emissive impurities (Fig. 2 and Fig. S20, SI).

The fluorescence quantum yields (Table 1) of cycloadducts **3** and **4** were determined by the internal reference method in DMF using 5,10,15,20-tetraphenylporphyrin (**TPP**, Φ_F= 0.11 in DMF) as reference. Compounds **3** and **4** show a slightly weaker emission when compared with the **TPP** used as reference. This fact can be due to the quenching of the excited singlet state by the uracil-alditol linked at the *beta*-pyrrolic position of the macrocycle. However, the values of Φ_{Flu} for derivatives **3-Xyl,-Gal** and **4-Xyl,-Gal** are not significantly affected by the presence of the different uracil-alditol moieties.

Table 1. Photophysical data of cycloadducts **3** and **4** obtained in DMF and at 293 K.

Compound	λ_{max} (log ε) / nm	λ_{em} / nm	Stokes shift / nm	Φ_{Flu} / %[a]
3-Xyl	419 (5.62) 516 (4.51) 554 (4.15) 592 (4.04) 647 (3.89)	655, 717	7	9
3-Gal	420 (5.73) 515 (4.50) 552 (4.16) 592 (4.04) 650 (3.92)	653, 718	3	9
4-Xyl	419 (5.44) 514 (4.54) 553 (4.19) 591 (4.08) 649 (3.88)	651, 714	2	8
4-Gal	419 (5.56) 515 (4.54) 551 (4.19) 591 (4.07) 648 (3.87)	653, 716	5	8

[a] **TPP (Φ_{Flu} = 11%) was used as reference.**

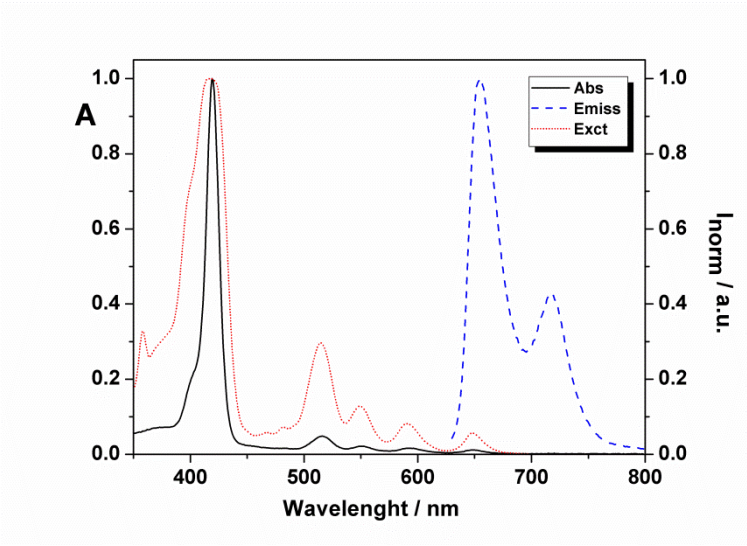

Fig. 2. Normalized absorption, emission and excitation spectra of compound **3-Xyl** in DMF at 293 K ($\lambda_{exc3\text{-}Xyl}$ = 516 nm and $\lambda_{em3\text{-}Xyl}$ = 717 nm).

The ability of these conjugates to generate $^1O_2$ was evaluated since it is also an important feature to take into account before hypothesizing their use as PDT PSs. Under this context, their efficacy to generate $^1O_2$ was qualitatively assessed by using an indirect method based on DPiBF photo-oxidation [51,52]. The generated $^1O_2$ reacts with the yellow DPiBF (λ_{max} 415 nm) in a [4+2] cycloaddition process, affording a colourless oxidized product. The results obtained show that all adducts are able to produce $^1O_2$, although

with a slightly slower rate than the well-known $^1O_2$ producer, **TPP** (Fig. 3). We also observed that cycloadducts **3** are slightly better $^1O_2$ producers than cycloadducts **4**. It is worth referring to the fact that the decay of DPiBF just occurred when the DPiBF solution was irradiated in the presence of the porphyrinic derivatives, which clearly indicates their role in the $^1O_2$ generation. Based on the promising photophysical properties of the new cycloadducts, a preliminary evaluation of their photodynamic action towards prostate cancer cells was undertaken.

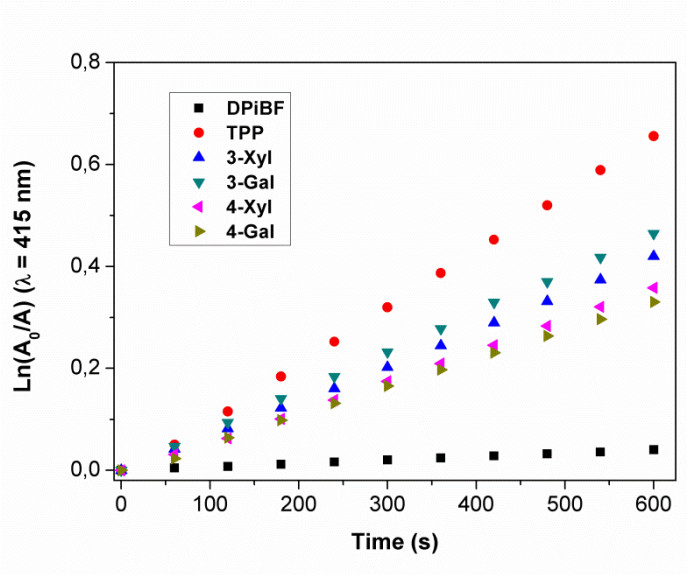

Fig. 3. Photo-oxidation of DPiBF in DMF photosensitized by compounds **3-Xyl, 3-Gal**, **4-Xyl, 4-Gal** and **TPP** during 600 s at 630 ± 20 nm at an irradiance of 4.0 mW cm^{-2}.

3.3. Biological Assays

The prostate is an interesting target organ for PDT [21], since prostate cancer is often locally confined and there are procedures for the interstitial administration of radiation that are adequately adapted [53]. The cytotoxic and phototoxic activities of the conjugates **3** and **4** were assessed against a human prostate cell line, PC-3 (prostatic adenocarcinoma cells, grade IV). The biological assessment was performed at concentrations 1.0, 10 and 100 µM in the dark and after exposing the cells to red light (630 ± 20 nm) for 20 min at an irradiance of 1.28 mW cm^{-2}. The results obtained (Fig. 4) show that all compounds do not present any cytotoxicity in the dark, since no significant decrease in cell viability was observed after 24 h of incubation (Fig. 4) ($p > 0.05$). When the cells were exposed to a red light it was possible to observe that only conjugates **4** present phototoxicity at the highest tested concentration (100 µM) ($p < 0.05$). At this concentration the cycloadducts **3** with the protected uracil-alditols moieties did not show any toxicity ($p > 0.05$). Besides, among compounds **4**, their efficiency to reduce the viability of PC-3 cells, seems to be

dependent on the sugar moiety since the galactose conjugate **4-Gal** showed higher efficiency than the xylose conjugate **4-Xyl**. There are some studies that reveal that the presence of galactose moieties in the structure of the molecules can improve photodynamic efficiency [37,54,55]. This is probably due to the fact that tumoral cells have galectins, and these proteins have carbohydrate recognition domains that bind specifically to β-galactoside sugars, resulting in a higher specificity and uptake of the PS by the tumour tissue [36]. In fact, PC-3 as well as other prostate tumoral cells expresses several members of the galectin family of proteins, which have been implicated in prostate cancer development and progression [56]. PC-3 cells express galectin-1 (the most abundant), galectin-3, galectin-8 and other members, though at lower expression levels [56].

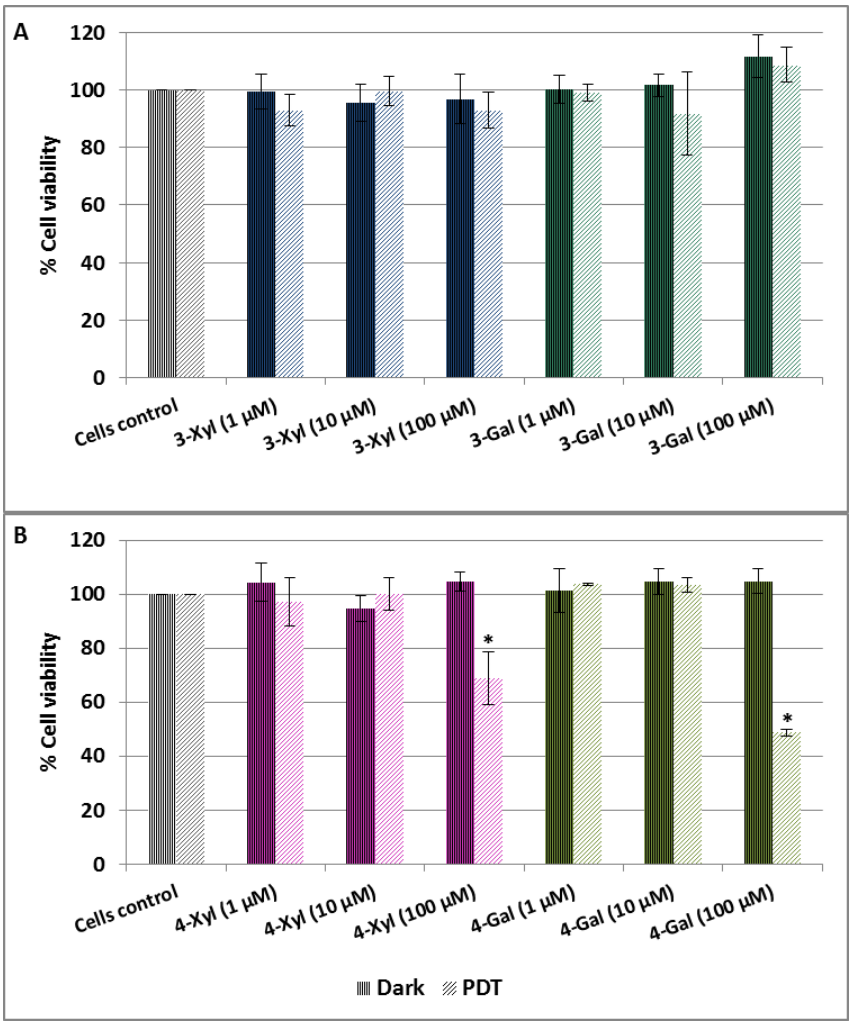

Fig. 4. Viability of PC-3 cells treated with the tested PS non-irradiated and irradiated with red light (1.28 mW cm^{-2}, 630±20 nm) for 20 min. **A.** Cycloadducts **3-Xyl,-Gal** and **B.** Cycloadducts **4-Xyl,-Gal** at 1.0, 10 and 100 µM. Values are the mean of three independent assays. The error bars represent the standard deviation of three independent experiments.

4. Conclusion

In conclusion, we have developed an efficient access to *meso*-tetraarylporphyrins bearing protected and unprotected uracil-alditol units at β-pyrrolic positions. The photophysical properties displayed by the prepared conjugates associated to their photodynamic efficiency against prostate cancer cell line (PC-3) are encouraging and further studies on the development these type of conjugates as photoactive molecules towards cancer will be performed.

Acknowledgments

Thanks are due to the University of Aveiro and FCT/MEC for the financial support to QOPNA (FCT UID/QUI/00062/2019) and Institute for Biomedicine – iBiMED (UID/BIM/04501/2013 and POCI-01-0145-FEDER-007628) research units, and to the FCT projects (FCT-PTDC/ASP-PES/29576/2017), through national funds and where applicable co-financed by the FEDER-Operational Thematic Program for Competitiveness and Internationalization-COMPETE 2020, within the PT2020 Partnership Agreement. Thanks are also due to the Portuguese NMR and Mass Networks. Cristina J Dias also thanks FCT for her research grant (BI/UI51/8448/2018). The research contract of N.M.M. Moura (REF.-048-88-ARH/2018) is funded by national funds (OE), through FCT – Fundação para a Ciência e a Tecnologia, I.P., in the scope of the framework contract foreseen in the numbers 4, 5 and 6 of the article 23, of the Decree-Law 57/2016, of August 29, changed by Law 57/2017, of July 19. JF was supported by an individual grant from FCT of the Portuguese Ministry of Science and Higher Education (SFRH/BD/102981/2014).

References

[1] Milgrom LR. The colours of life. Oxford University Press: Oxford, 1997.

[2] Kadish KM, Smith KM, Guilard R. Handbook of porphyrin science. World Scientific Publishing Company: Singapore, 2010.

[3] Almeida A, Cunha A, Faustino MAF, Tomé AC, Neves MGPMS. Porphyrins as Antimicrobial Photosensitizing Agents in "Photodynamic Inactivation of Microbial Pathogens: Medical and Environmental Applications." In: Hamblin MR, Jori G, editors., 2011.

[4] Urbani M, Grätzel M, Nazeeruddin MK, Torres T. Meso-Substituted Porphyrins for Dye-Sensitized Solar Cells. Chem Rev 2014;114:12330–96. doi:10.1021/cr5001964.

[5] Mesquita MQ, Menezes JC, Pires SMG, Neves MG, Simões MMQ, Tomé AC, Cavaleiro JAS, Cunha Â, Daniel-da-Silva AL, Almeida A. Pyrrolidine-fused chlorin photosensitizer immobilized on solid supports for the photoinactivation of Gram negative bacteria. Dyes Pigments 2014;110:123–33. doi:10.1016/j.dyepig.2014.04.025.

411 [6] Tanaka T, Osuka A. Conjugated porphyrin arrays: Synthesis, properties and applications for functional
412 materials. Chem Soc Rev 2015;44:943–69. doi:10.1039/c3cs60443h.
413 [7] Paolesse R, Nardis S, Monti D, Stefanelli M, Di Natale C. Porphyrinoids for Chemical Sensor Applications.
414 Chem Rev 2017;117:2517–83. doi:10.1021/acs.chemrev.6b00361.
415 [8] Baglia RA, Zaragoza JPT, Goldberg DP. Biomimetic Reactivity of Oxygen-Derived Manganese and Iron
416 Porphyrinoid Complexes. Chem Rev 2017;117:13320–52. doi:10.1021/acs.chemrev.7b00180.
417 [9] Zhang W, Lai W, Cao R. Energy-Related Small Molecule Activation Reactions: Oxygen Reduction and
418 Hydrogen and Oxygen Evolution Reactions Catalyzed by Porphyrin- and Corrole-Based Systems. Chem Rev
419 2017;117:3717–97. doi:10.1021/acs.chemrev.6b00299.
420 [10] Castro KADF, Moura NMM, Fernandes A, Faustino MAF, Simões MMQ, Cavaleiro JAS,Nakagaki S, Almeida
421 A, Cunha Â, Silvestre AJD, Freire C, Pinto RJB, Neves MGPMS. Control of Listeria innocua biofilms by
422 biocompatible photodynamic antifouling chitosan based materials. Dyes Pigments 2017;137:265–76.
423 doi:10.1016/j.dyepig.2016.10.020.
424 [11] Marciel L, Teles L, Moreira B, Pacheco M, Lourenço LMO, Neves MG, Tomé JPC, Faustino MAF, Almeida A.
425 An effective and potentially safe blood disinfection protocol using tetrapyrrolic photosensitizers. Future
426 Med Chem 2017;9:365–79. doi:10.4155/fmc-2016-0217.
427 [12] Diogo P, Fernandes C, Caramelo F, Mota M, Miranda IM, Faustino MAF,Neves MGPMS, de Oliveira KT,
428 Santos JM, Gonçalves T. Antimicrobial Photodynamic Therapy against Endodontic Enterococcus faecalis
429 and Candida albicans Mono and Mixed Biofilms in the Presence of Photosensitizers: A Comparative Study
430 with Classical Endodontic Irrigants. Front Microbiol 2017;8:498. doi:10.3389/fmicb.2017.00498.
431 [13] Otsuki J. Supramolecular approach towards light-harvesting materials based on porphyrins and
432 chlorophylls. J Mater Chem A 2018;6:6710–53. doi:10.1039/c7ta11274b.
433 [14] Branco TM, Valério NC, Jesus VIR, Dias CJ, Neves MGPMS, Faustino MAF, Almeida A. Single and combined
434 effects of photodynamic therapy and antibiotics to inactivate Staphylococcus aureus on skin.
435 Photodiagnosis Photodyn Ther 2018, 21:285-93. doi:https://doi.org/10.1016/j.pdpdt.2018.01.001.
436 [15] Abrahamse, H; Hamblin M. New photosensitizers for photodynamic therapy. Biochem J 2016;473:347–64.
437 doi:10.1042/BJ20150942.
438 [16] Alves E, Faustino MAF, Neves MG, Cunha Â, Nadais H, Almeida A. Potential applications of porphyrins in
439 photodynamic inactivation beyond the medical scope. J Photochem Photobiol C Photochem Rev
440 2015;22:34–57. doi:10.1016/j.jphotochemrev.2014.09.003.
441 [17] Rajora MA, Lou JWH, Zheng G. Advancing porphyrin's biomedical utility: Via supramolecular chemistry.
442 Chem Soc Rev 2017;46:6433–69. doi:10.1039/c7cs00525c.

[18] Mesquita MQ, Dias CJ, Gamelas S, Fardilha M, Neves MGPMS, Faustino MAF. An insight on the role of photosensitizer nanocarriers for Photodynamic Therapy. Ann Brazilian Acad Sci 2018;90:1101–30. doi:10.1590/0001-3765201720170800.

[19] Mesquita MQ, Dias CJ, Neves MGPMS, Almeida A, Faustino MAF. Revisiting current photoactive materials for antimicrobial photodynamic therapy. Molecules 2018;23. doi:10.3390/molecules23102424.

[20] Frochot C, Mordon S. Update of the situation of clinical photodynamic therapy in Europe in the 2003-2018 period. J Porphyr Phthalocyanines 2019;23:347–57. doi:10.1142/S1088424619300027.

[21] Gheewala T, Skwor T, Munirathinam G. Photosensitizers in prostate cancer therapy. Oncotarget 2017;8:30524–38. doi:10.18632/oncotarget.15496.

[22] Dolmans DEJGJ, Fukumura D, Jain RK. Photodynamic therapy for cancer. Nat Rev Cancer 2003;3:380–7. doi:10.1038/nrc1070.

[23] DeRosa MC, Crutchley RJ. Photosensitized singlet oxygen and its applications. Coord Chem Rev 2002:351–71. doi:10.1016/S0010-8545(02)00034-6.

[24] Serra VV, Zamarrón A, Faustino MAF, Cruz MCID La, Blázquez A, Rodrigues JMM, Neves MGPMS, Cavaleiro JAS, Juarranz A, Sanz-Rodríguez F. New porphyrin amino acid conjugates: Synthesis and photodynamic effect in human epithelial cells. Bioorganic Med Chem 2010;18:6170–8. doi:10.1016/j.bmc.2010.06.030.

[25] Gomes ATPC, Faustino MAF, Neves MGPMS, Ferreira VF, Juarranz A, Cavaleiro JAS, Sanz-Rodríguez F. Photodynamic effect of glycochlorin conjugates in human cancer epithelial cells. RSC Adv 2015;5:33496–502. doi:10.1039/C5RA04345J.

[26] Pałasz A, Ciez D. In search of uracil derivatives as bioactive agents. Uracils and fused uracils: Synthesis, biological activity and applications. Eur J Med Chem 2015;97:582–611. doi:10.1016/j.ejmech.2014.10.008.

[27] Bhosle MR, Khillare LD, Mali JR, Sarkate AP, Lokwani DK, Tiwari SV. DIPEAc promoted one-pot synthesis of dihydropyrido[2,3-*d*::6,5-*d'*]dipyrimidinetetraone and pyrimido[4,5-*d*] pyrimidine derivatives as potent tyrosinase inhibitors and anticancer agents: *in vitro* screening, molecular docking and ADMET predictions. New J Chem 2018;42:18621–32. doi:10.1039/c8nj04622k.

[28] Singh A, Lumb I, Mehra V, Kumar V. Ferrocene-appended pharmacophores: an exciting approach for modulating the biological potential of organic scaffolds. Dalt Trans 2019:2840–60. doi:10.1039/c9dt90027f.

[29] Shi X, Barkigia KM, Fajer J, Drain CM. Design and synthesis of porphyrins bearing rigid hydrogen bonding motifs: Highly versatile building blocks for self-assembly of polymers and discrete arrays. J Org Chem 2001;66:6513–22. doi:10.1021/jo010108c.

[30] Arai S, Niwa D, Nishide H, Takeoka S. Atropisomers of meso-conjugated uracyl porphyrin derivatives and their assembling structures. Org Lett 2007;9:17–20. doi:10.1021/ol062394q.

475 [31] Carvalho CMB, Fujita MA, Brocksom TJ, De Oliveira KT. Synthesis and photophysical evaluations of B-fused
476 uracil-porphyrin derivatives. Tetrahedron 2013;69:9986–93. doi:10.1016/j.tet.2013.09.069.
477 [32] Weimin S, Gen Z, Guifu D, Yunxiao Z, Jin Z, Jingchao T. Synthesis and *in vitro* PDT activity of miscellaneous
478 porphyrins with amino acid and uracil. Bioorganic Med Chem 2008;16:5665–71.
479 doi:10.1016/j.bmc.2008.03.063.
480 [33] Singh S, Aggarwal A, Bhupathiraju NVSDK, Arianna G, Tiwari K, Drain CM. Glycosylated Porphyrins,
481 Phthalocyanines, and Other Porphyrinoids for Diagnostics and Therapeutics. Chem Rev 2015;115:10261–
482 306. doi:10.1021/acs.chemrev.5b00244.
483 [34] Abdel-Aal MT. Synthesis and anti-hepatitis B activity of new substituted uracil and thiouracil glycosides.
484 Arch Pharm Res 2010;33:797–805. doi:10.1007/s12272-010-0601-y.
485 [35] Li G, Pandey SK, Graham A, Dobhal MP, Mehta R, Chen Y, Gryshuk A, Rittenhouse-Olson K, Oseroff A,
486 Pandey RK. Functionalization of OEP-Based Benzochlorins to Develop Carbohydrate-Conjugated
487 Photosensitizers. Attempt to Target β -Galactoside-Recognized Proteins. J Org Chem 2004;69:158–72.
488 doi:10.1021/jo030280b.
489 [36] Zheng X, Pandey RK. Porphyrin-Carbohydrate Conjugates: Impact of Carbohydrate Moieties in
490 Photodynamic Therapy (PDT). Anticancer Agents Med Chem 2008;8:241–68. doi:
491 10.2174/187152008783961897.
492 [37] Pereira PMR, Silva S, Cavaleiro JAS, Ribeiro CAF, Tomé JPC, Fernandes R. Galactodendritic phthalocyanine
493 targets carbohydrate-binding proteins enhancing photodynamic therapy. PLoS One 2014;9:22–30.
494 doi:10.1371/journal.pone.0095529.
495 [38] Pereira PMR, Silva S, Bispo M, Zuzarte M, Gomes C, Girão H, Cavaleiro JAS, Ribeiro CA, Tomé JPC,
496 Fernandes R. Mitochondria-targeted photodynamic therapy with a galactodendritic chlorin to enhance cell
497 death in resistant bladder cancer cells. Bioconjug Chem 2016;27:2762–9. doi:
498 10.1021/acs.bioconjchem.6b00519.
499 [39] Palasz A, Kalinowska-Tluscik J, Jablonski M. Application of 2,4,6-trioxo-pyrimidin-5-ylidene alditols in the
500 synthesis of pyrano [2,3-*d*] pyrimidines containing a sugar moiety by hetero-Diels-Alder reactions and by
501 conjugate Michael addition-cyclizations. Tetrahedron 2013;69:8216–27. doi:10.1016/j.tet.2013.07.032.
502 [40] Cavaleiro JAS, Tomé AC, Neves MGPMS. Meso-tetraarylporphyrin derivatives: New synthetic
503 methodologies. In Handbook of Porphyrin Science; Kadish, K.M., Smith, K.M., Guilard, R., Eds.; World
504 Scientific: Singapore, 2010; Volume 2, Chapter 9, pp. 193–294..
505 [41] Cavaleiro JAS, Neves MGPMS, Tome AC. Cycloaddition reactions of porphyrins. ARKIVOC , 2003 (xiv) 107-
506 130. doi:10.3998/ark.5550190.0004.e11.

[42] Tomé AC, Neves MGPMS, Cavaleiro JAS. Porphyrins and other pyrrolic macrocycles in cycloaddition reactions. J Porphyrins Phthalocyanines 2009;13:408–14. doi:10.1142/S1088424609000619.

[43] Cerqueira AFR, Almodôvar VAS, Neves MGPMS, Tomé AC. Coumarin–Tetrapyrrolic Macrocycle Conjugates: Synthesis and Applications. Molecules 2017;22:994. doi:10.3390/molecules22060994.

[44] Armarego WLF. Purification of laboratory chemicals. fourth ed. Oxford: Butterworth-Heinemann; 1996.

[45] Callot HJ. Nouvelles voies d'accès aux vinylporphyrines. Tetrahedron 1973;29:899–901. doi:https://doi.org/10.1016/0040-4020(73)80035-3.

[46] Moura NMM, Faustino MAF, Neves MGPMS, Tomé AC, Rakib M, Hannioui A, Mojahidi S, Hackbarth S, Röder B, Paz FAA, Silva A, Cavaleiro JAS. Novel pyrazoline and pyrazole porphyrin derivatives: synthesis and photophysical properties. Tetrahedron 2012;68:8181–93. doi:10.1016/j.tet.2012.07.072.

[47] Gonzalez MA, Requejo JLJ, Albarran JCP, Perez J. Facile preparation of C-glycosylbarbiturates and C-glycosylbarbituric acids. Carbohydr Res 1986;158:53–66. doi:https://doi.org/10.1016/0008-6215(86)84005-8.

[48] Hashimoto T, Choe Y-K, Nakano H, Hirao K. Theoretical Study of the Q and B Bands of Free-Base, Magnesium, and Zinc Porphyrins, and Their Derivatives. J Phys Chem A 2002;103:1894–904. doi:10.1021/jp984807d.

[49] Maximiano R V., Piovesan E, Zílio SC, MacHado AEH, De Paula R, Cavaleiro JAS, Borissevitch IE, Ito AS, Gonçalves PJ, Barbosa Neto NM. Excited-state absorption investigation of a cationic porphyrin derivative. J Photochem Photobiol A Chem 2010;214:115–20. doi:10.1016/j.jphotochem.2010.06.007.

[50] Baskin JS, Yu HZ, Zewail AH. Ultrafast dynamics of porphyrins in the condensed phase: I. Free base tetraphenylporphyrin. J Phys Chem A 2002;106:9837–44. doi:10.1021/jp020398g.

[51] Spiller W, Kliesch H, Wöhrle D, Hackbarth S, Röder B, Schnurpfeil G. Singlet Oxygen Quantum Yields of Different Photosensitizers in Polar Solvents and Micellar Solutions. J Porphyr Phthalocyanines 1998;2:145–58. doi: 10.1002/(SICI)1099-1409(199803/04)2:2<145::AID-JPP60>3.0.CO;2-2.

[52] Zenkevich E, Sagun E, Knyukshto V, Shulga A, Mironov A, Efremova O, Bonnet R, Songca SP, Kassem M. Photophysical and photochemical properties of potential porphyrin and chlorin photosensitizers for PDT. J Photochem Photobiol B Biol 1996;33:171–80. doi:10.1016/1011-1344(95)07241-1.

[53] Zhu TC, Finlay JC. Prostate PDT dosimetry. Photodiagnosis Photodyn Ther 2006;3:234–46. doi:10.1016/j.pdpdt.2006.08.002.

[54] Zheng G, Graham A, Shibata M, Missert JR, Oseroff AR, Dougherty TJ,Pandey RK. Synthesis of β-galactose-conjugated chlorins derived by enyne metathesis as galectin-specific photosensitizers for photodynamic therapy. J Org Chem 2001;66:8709–16. doi:10.1021/jo0105080.

[55] Lee PPS, Lo PC, Chan EYM, Fong WP, Ko WH, Ng DKP. Synthesis and *in vitro* photodynamic activity of novel galactose-containing phthalocyanines. Tetrahedron Lett 2005;46:1551–4. doi:10.1016/j.tetlet.2004.12.137.

[56] Laderach DJ, Gentilini L, Jaworski FM, Compagno D. Galectins as new prognostic markers and potential therapeutic targets for advanced prostate cancers. Prostate Cancer 2013;2013:519436. doi: 10.1155/2013/519436.